Joint Center for Satellite Data Assimilation

Office Note (unassigned)

This is an unreviewed manuscript, primarily intended for informal exchange of information among JCSDA researchers

CRTM: AVHRR Infrared Spectral Response Function Comparison

Paul van Delst[a] , David Groff[b]
JCSDA/EMC/SAIC

November, 2008

---

[a]paul.vandelst@noaa.gov
[b]david.groff@noaa.gov

Change History

Date	Author	Change
2008-11-01	P.van Delst	Initial release.
2008-11-04	P.van Delst	Minor corrections from review.
2008-11-14	D.Groff	Added appendice for NOAA-16 cutoff issue.
2008-11-18	P.van Delst	Corrected all references to NOAA-17 SRF difference that were resolved when the correct datafiles were used. Moved NOAA-16 appendix into main document and added additional SRF wing plots.

1 Introduction

The CRTM project is preparing to recompute all of the instrument resolution transmittances (used in the transmittance model regression fitting) to take advantage of improved spectroscopy in line-by-line (LBL) models. Additionally, we are endeavouring to use only the spectral response function (SRF) data from “official” sources directly related to instrument development/calibration etc.

The AVHRR SRF data used to generate the *current* CRTM spectral (SpcCoeff) and transmittance model (TauCoeff) coefficients came from two sources: NOAA-15 to NOAA-17 AVHRR SRFs came from CIMSS/SSEC[1] [Woolf, H.M.]; NOAA-18 and MetOp-A AVHRR SRFs came from Sullivan, J.T. [2003] and Sullivan, J.T. [2006] respectively. The official source of the AVHRR SRF data we wish to use for future TauCoeff generation is the NOAA AVHRR Spectral Response Function website [Wu, X.].

This document describes the pre-processing during this transition period with respect to the AVHRR instrument infrared channels on the polar orbiter platforms NOAA-16, NOAA-17, NOAA-18, and MetOp-A. This lead us to question our pre-processing practices and to verify that SRF interpolation is not introducing any artifacts, such as a bias, in CRTM calculations.

[1]Cooperative Institute for Meteorological Satellite Studies/Space Science and Engineering Center, University of Wisconsin-Madison

2 AVHRR infrared channel SRFs

2.1 Gross SRF comparison

Plots of the SRF data for AVHRR channels 3B, 4, and 5 for the NOAA-16 to MetOp-A platforms are shown in appendix A. SRF plots for NOAA-16 are shown in figure A.1, NOAA-17 in figure A.2, NOAA-18 in figure A.3, and MetOp-A in figure A.4 respectively.

In general, at the scales shown, the SRFs shown in appendix A agree quite well. It is at higher magnifications of the SRF data that differences become visible.

2.2 Interpolation differences

The main source of differences between the SRFs is due to interpolation. For the AVHRR instruments, the channels responses are typically reported as a function of wavelength (μm). For the CRTM transmittance production process, we require the SRFs to be,

- A function of frequency (cm^{-1}).
- At a fixed frequency interval. For broadband infrared instruments, the frequency interval used is 0.1cm^{-1}.
- Begun on a 0.1cm^{-1} boundary such as 840.0, 900.6, etc.

As such, interpolation of the original data is required.

Our regular processing takes the original channel responses and interpolates the data using the IDL[2] `SPLINE` function with a tension value of 5.0, selected qualitatively. From the online IDL help[3]:

> If [the tension value] is close to 0, (e.g., .01), then effectively there is a cubic spline fit. If [the tension value] is large, (e.g., greater than 10), then the fit will be like a polynomial interpolation.

The impacts of the interpolation scheme are shown visually in figures 2.1 and 2.2 for NOAA-16 AVHRR/3 channels 3 and 5; figures 2.3 and 2.4 for NOAA-17 AVHRR/3 channels 4 and 5; figures 2.5 and 2.6 for NOAA-18 AVHRR/3 channels 3 and 4; and in figures 2.7 and 2.8 for MetOp-A AVHRR/3 channels 3 and 5. Only two channels from each instrument are shown with the understanding that the third channel exhinbits the same sort of differences.

For both the NOAA-16 and NOAA-17 instruments, the current SRF data was linearly interpolated from a much lower resolution dataset, and subsequent spline interpolations have little effect. The impact of the spline interpolation on the lower resolution official SRF data is clearly evident. Note also that there is a slight vertical extent difference between the current and official SRF data – this is most likely due to renormalisation of the SRFs.

In the NOAA-18 AVHRR/3 case, the SRF datasets coincide almost exactly. The differences that do remain can be attributed to the number of decimal places to which the original and intermediate data was reported in ASCII datafiles.

The current SRF data used for MetOp-A AVHRR/3 clearly suffers from quantisation of the data in the original ASCII datafile (reported to only three decimal places). This data was supplied directly by ITT [Sullivan, J.T., 2006] and, at the time, was the only data available. The offical SRF data from Wu, X. is listed as being modified on 04/21/2008, but it is not yet known if those modifications addressed the quantisation problem.

[2] Interactive Data Language; a scripting language that provides various functionalities for data processing and visualisation

[3] IDL Reference Guide; for IDL Version 7.0, November 2007 Edition, see pp2346-2347; Note the download file is quite large.

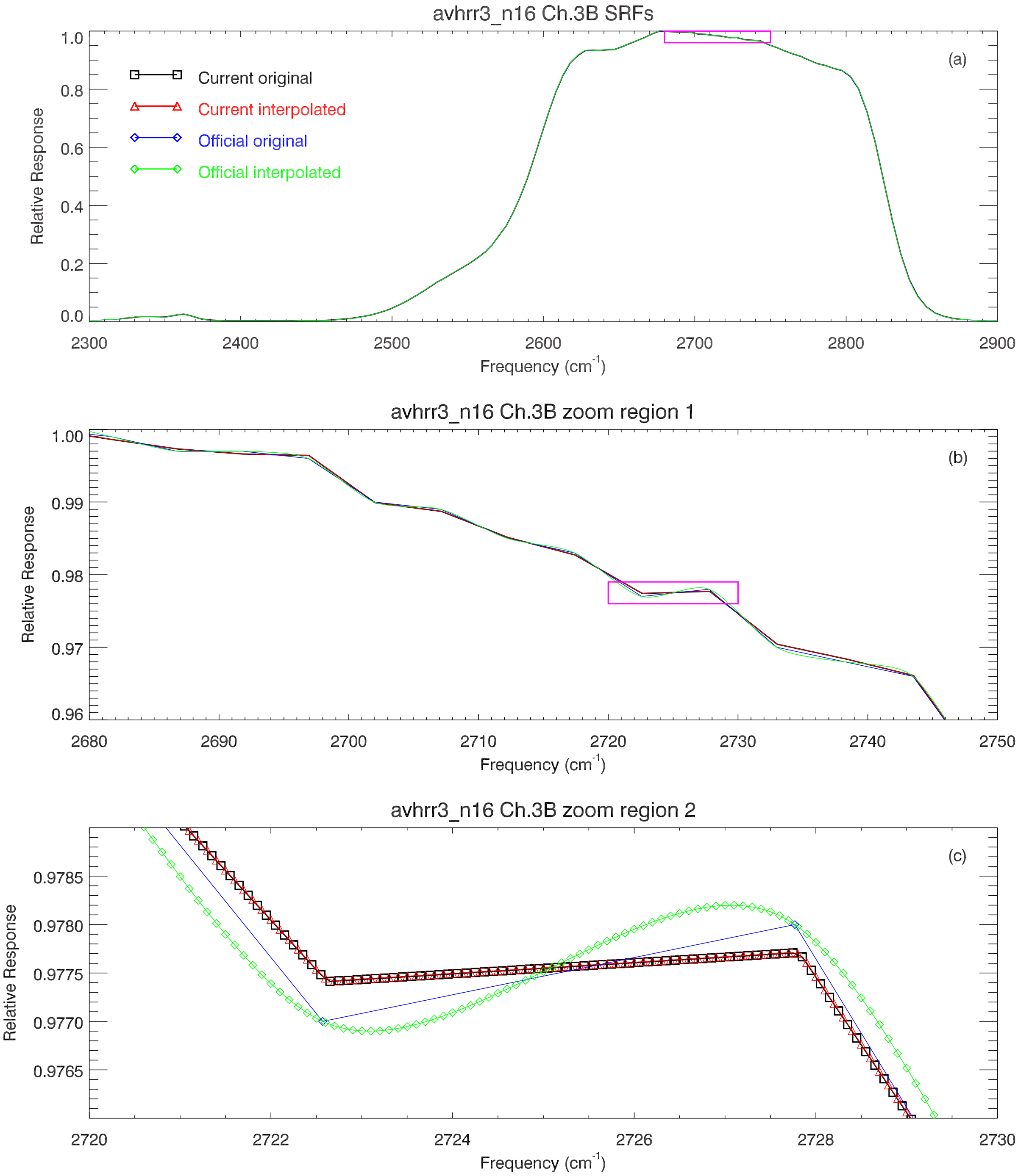

Figure 2.1: Zoom of NOAA-16 AVHRR/3 channel 3B SRF comparison. **(a)** Complete SRFs showing zoom region 1. **(b)** Magnification of SRF section from (a) showing zoom region 2. **(c)** Magnification of SRF section from (b).

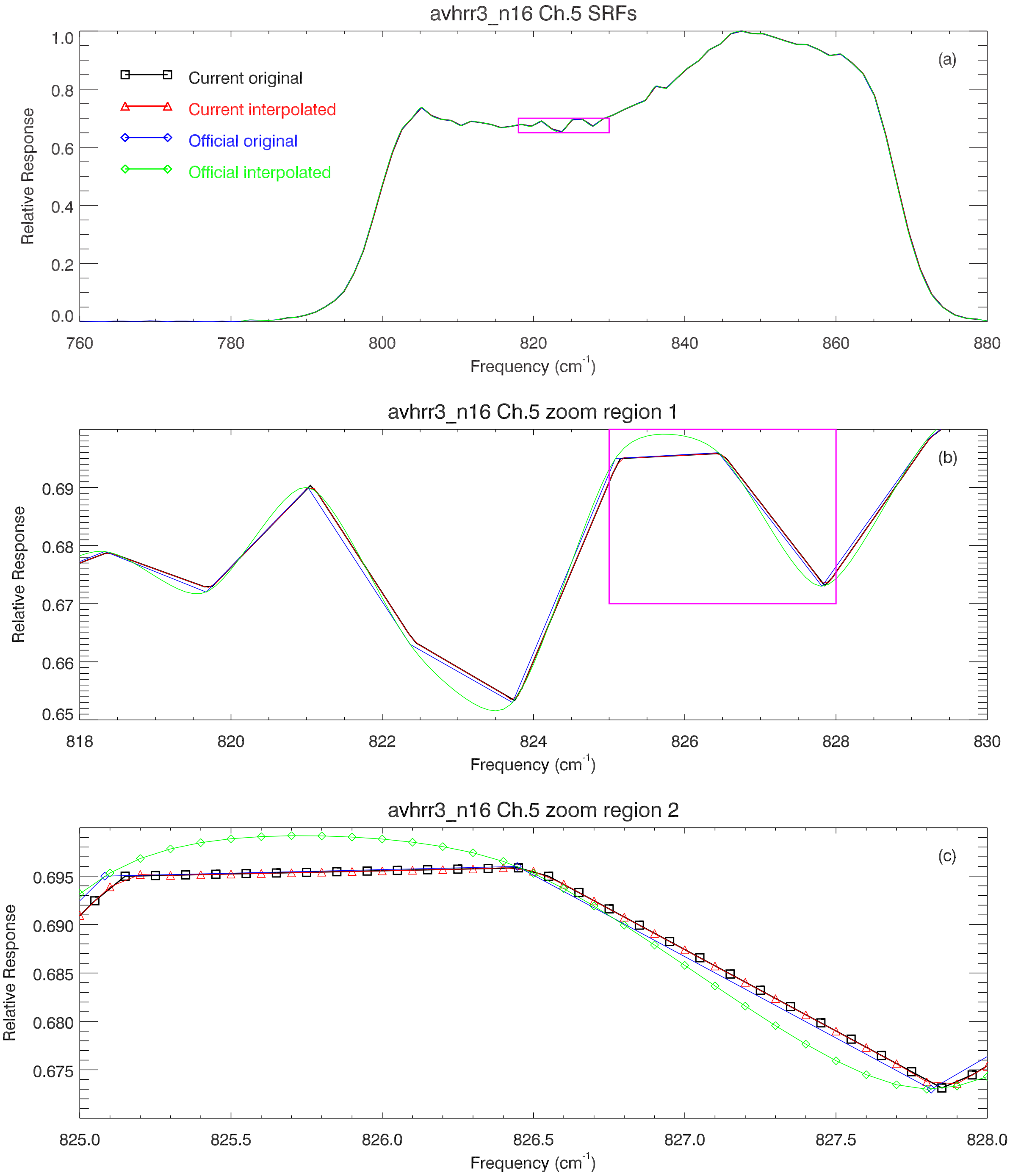

Figure 2.2: Zoom of NOAA-16 AVHRR/3 channel 5 SRF comparison. **(a)** Complete SRFs showing zoom region 1. **(b)** Magnification of SRF section from (a) showing zoom region 2. **(c)** Magnification of SRF section from (b).

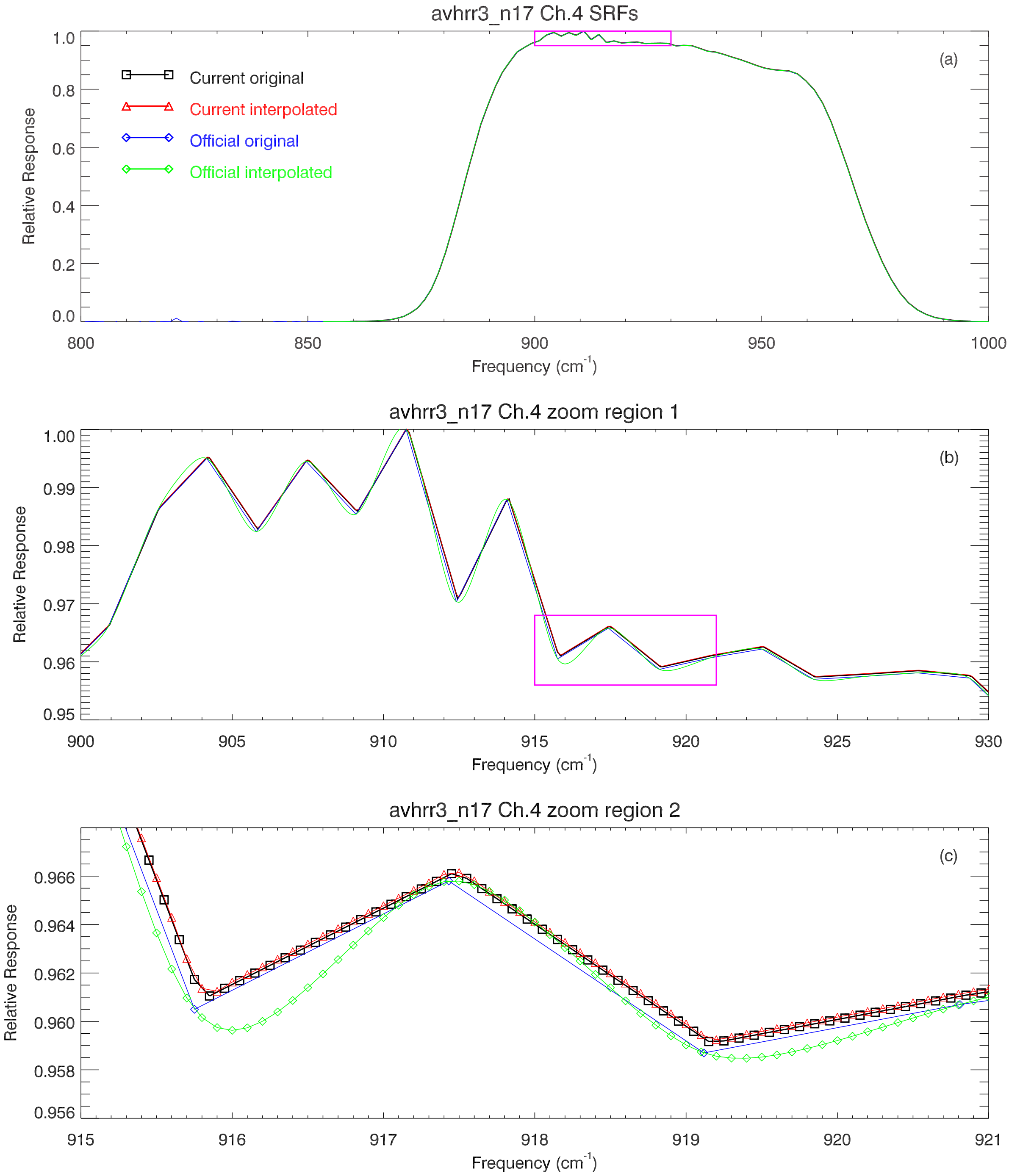

Figure 2.3: Zoom of NOAA-17 AVHRR/3 channel 4 SRF comparison. **(a)** Complete SRFs showing zoom region 1. **(b)** Magnification of SRF section from (a) showing zoom region 2. **(c)** Magnification of SRF section from (b).

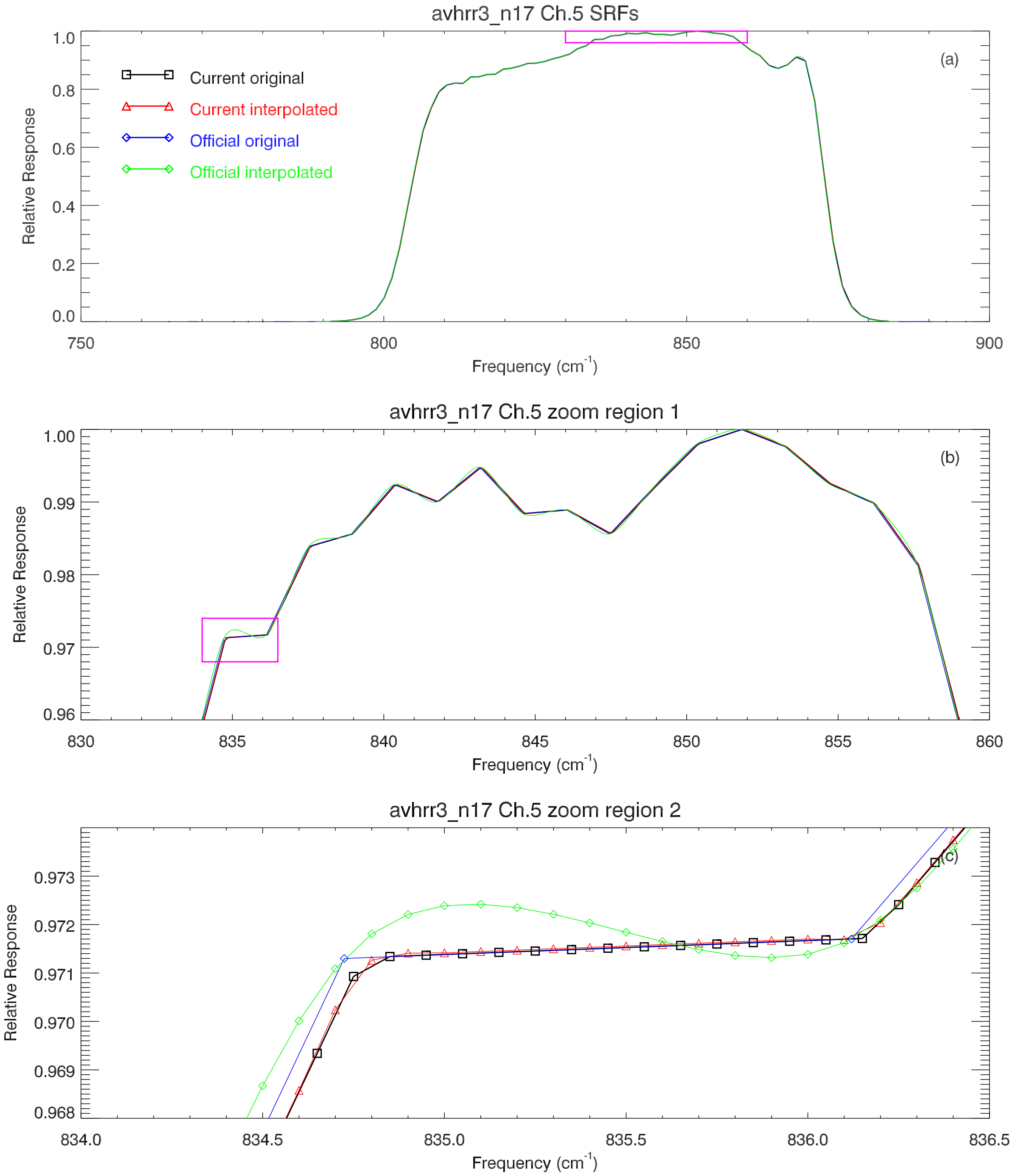

Figure 2.4: Zoom of NOAA-17 AVHRR/3 channel 5 SRF comparison. **(a)** Complete SRFs showing zoom region 1. **(b)** Magnification of SRF section from (a) showing zoom region 2. **(c)** Magnification of SRF section from (b).

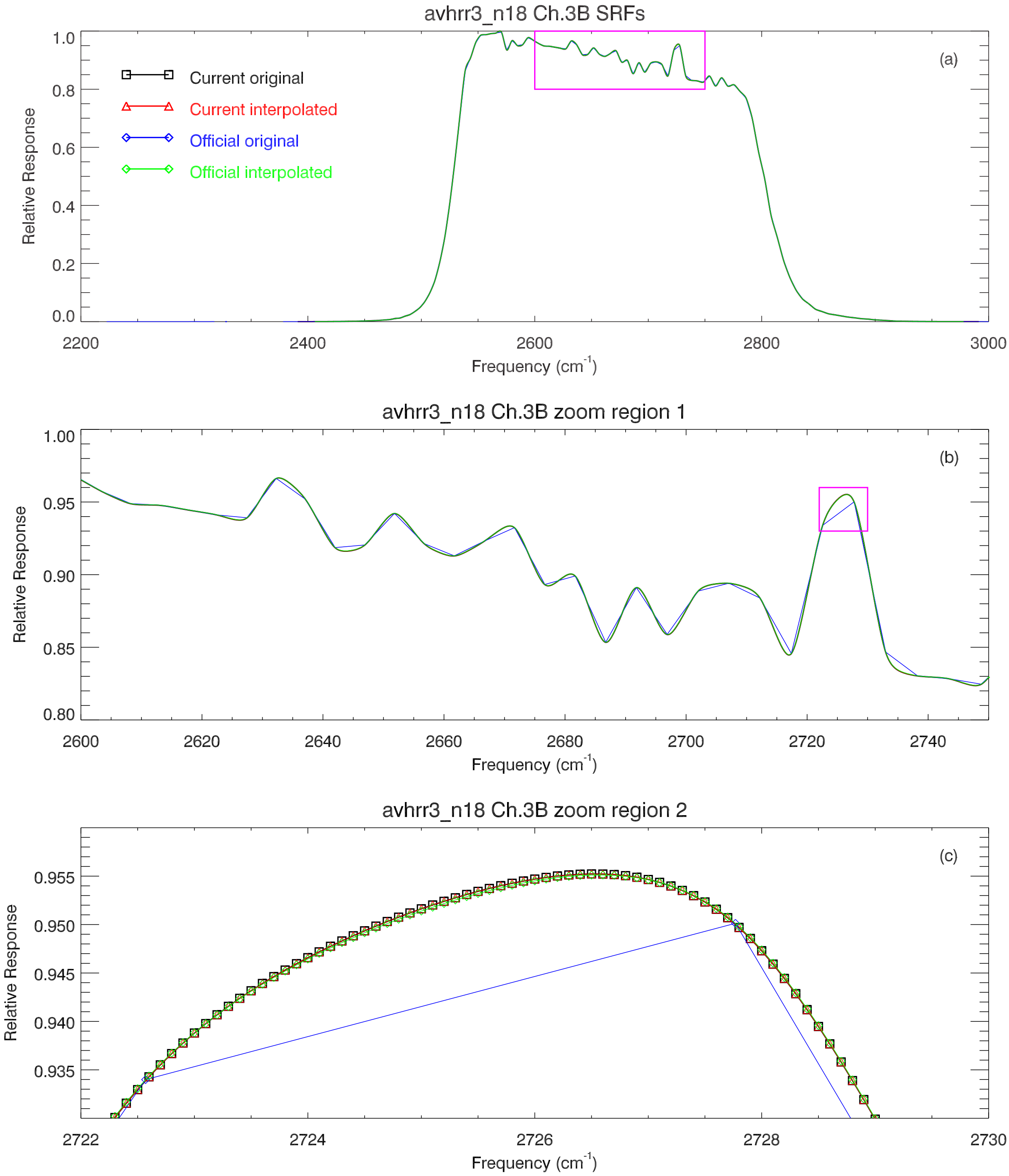

Figure 2.5: Zoom of NOAA-18 AVHRR/3 channel 3B SRF comparison. **(a)** Complete SRFs showing zoom region 1. **(b)** Magnification of SRF section from (a) showing zoom region 2. **(c)** Magnification of SRF section from (b).

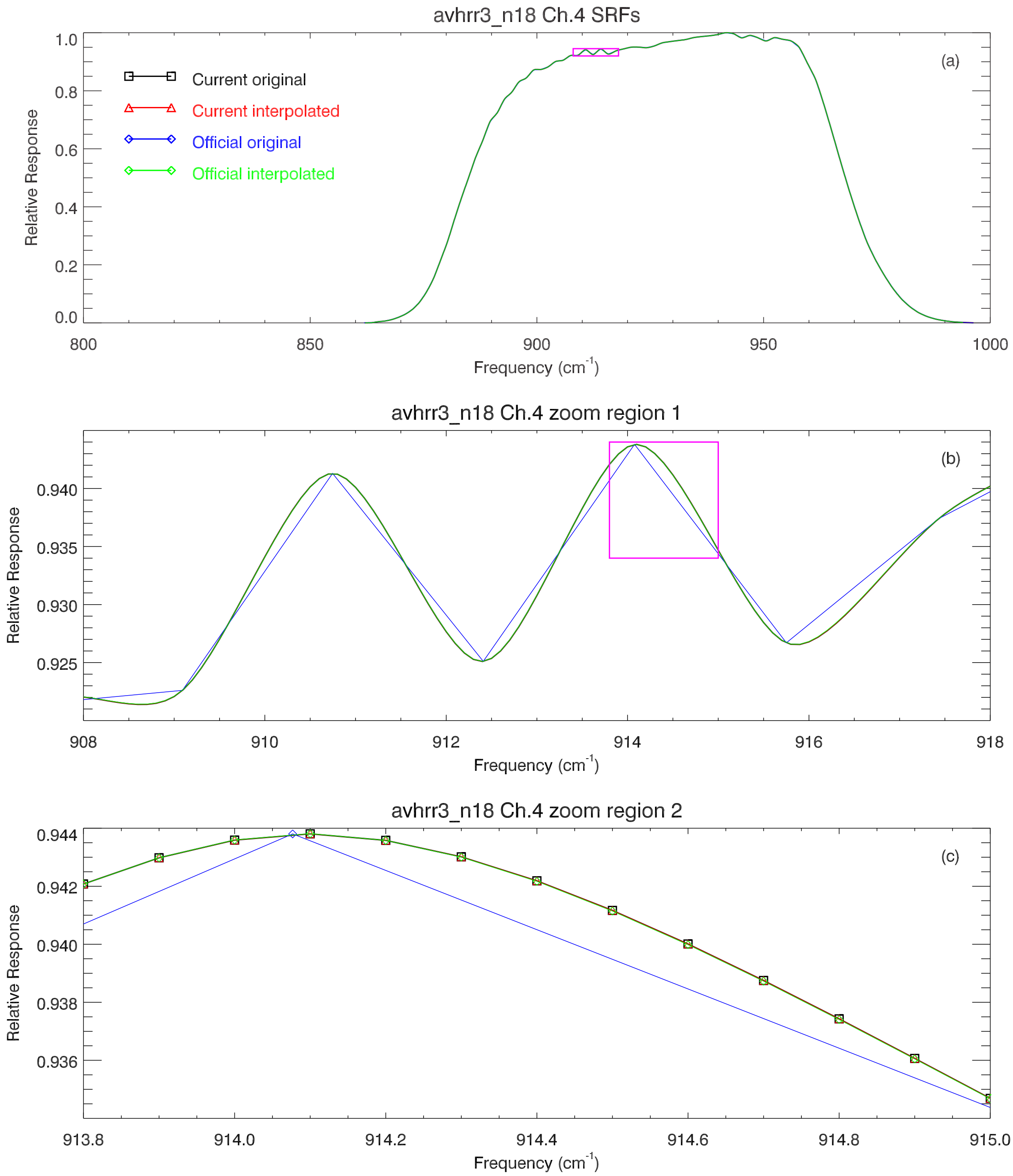

Figure 2.6: Zoom of NOAA-18 AVHRR/3 channel 4 SRF comparison. **(a)** Complete SRFs showing zoom region 1. **(b)** Magnification of SRF section from (a) showing zoom region 2. **(c)** Magnification of SRF section from (b).

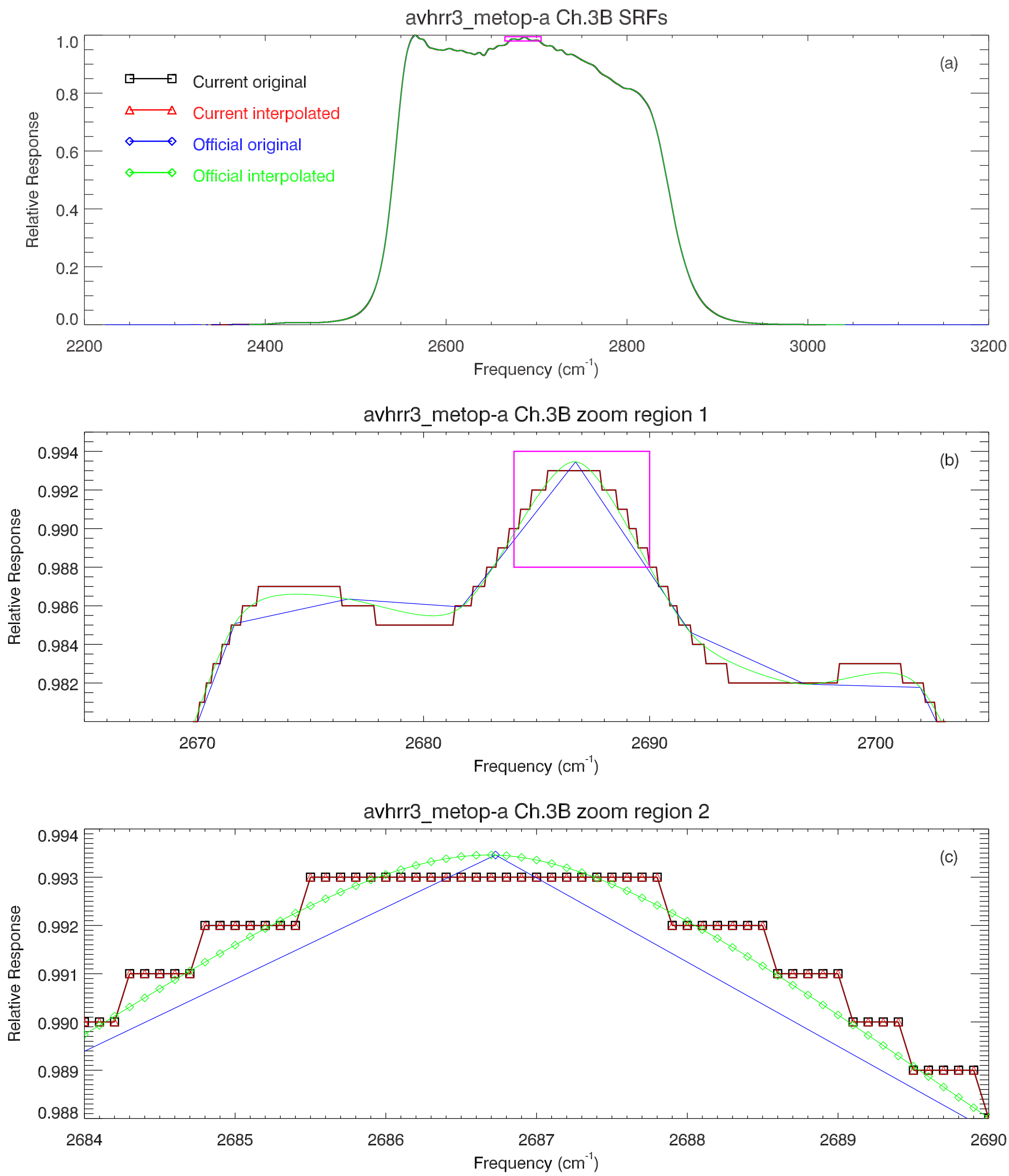

Figure 2.7: Zoom of MetOp-A AVHRR/3 channel 3B SRF comparison. **(a)** Complete SRFs showing zoom region 1. **(b)** Magnification of SRF section from (a) showing zoom region 2. **(c)** Magnification of SRF section from (b).

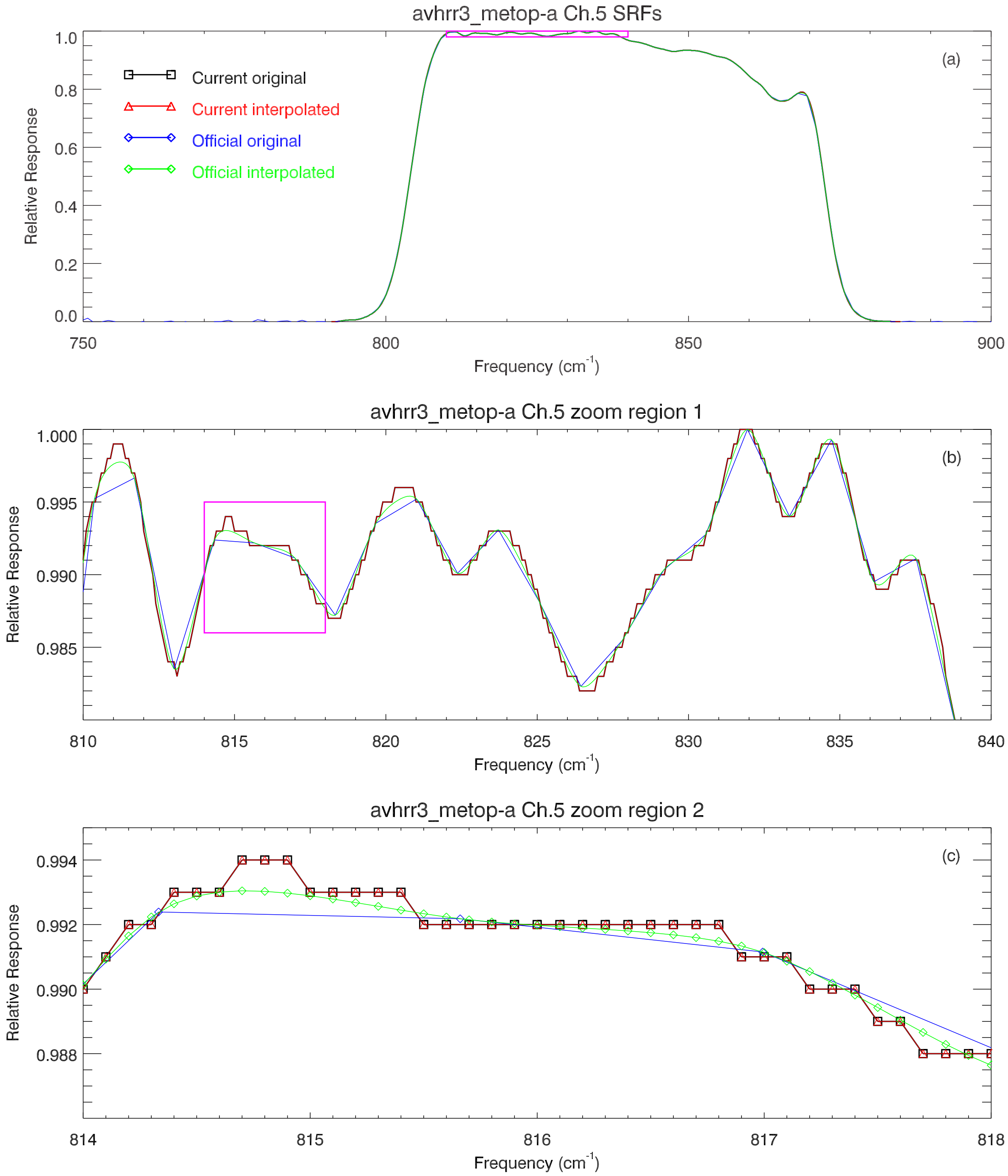

Figure 2.8: Zoom of MetOp-A AVHRR/3 channel 5 SRF comparison. **(a)** Complete SRFs showing zoom region 1. **(b)** Magnification of SRF section from (a) showing zoom region 2. **(c)** Magnification of SRF section from (b).

3 Radiometric impact of SRF interpolation

To determine the radiometric impact of the various forms of the SRF (due to different data sources or different interpolation methods), effective temperatures[4] for each sensor channel were computed for a blackbody temperature of 285K. The result for the spline interpolated SRF with a tension of 5.0 (spline5) was chosen as the reference. Comparisons were then made with results for a linearly interpolated SRF (linear), a spline interpolated SRF with tension of 0.1 (spline0.1), a spline interpolated SRF with tension of 20 (spline20), the original uninterpolated SRF itself (original), and the current SRF used in CRTM processing (current). The temperature residuals for an SRF type, "x", are defined as,

$$\Delta T(\text{x}) = T_{eff}(\text{spline5}) - T_{eff}(\text{x}) \tag{3.1}$$

and are shown in table 3.1. It is apparent that the type of interpolation used on the SRFs has minimal radiometric impact.

The computed central frequencies and band correction coefficients for the NOAA-16, -17, -18, and MetOp-A AVHRR sensors are shown in appendix B.

Platform	**Channel**	T_{eff} spline5 (K)	ΔT linear (K)	ΔT spline0.1 (K)	ΔT spline20 (K)	ΔT original (K)	ΔT current (K)
NOAA-16	3B	286.12	-4.72e-04	2.04e-04	-3.05e-04	1.51e-04	2.92e-02
	4	285.01	-3.43e-06	1.73e-06	-2.28e-06	1.76e-06	1.26e-05
	5	284.98	8.93e-06	-3.44e-06	5.68e-06	-4.33e-06	-8.88e-05
NOAA-17	3B	286.07	-4.73e-04	1.75e-04	-2.99e-04	1.74e-04	1.35e-04
	4	285.01	-4.91e-06	2.18e-06	-3.19e-06	2.17e-06	-2.03e-05
	5	284.98	9.74e-06	-3.51e-06	6.16e-06	-3.42e-06	-1.07e-05
NOAA-18	3B	286.10	-4.71e-04	1.72e-04	-2.97e-04	1.72e-04	-8.32e-05
	4	285.01	-4.95e-06	2.20e-06	-3.22e-06	2.22e-06	-4.60e-06
	5	284.98	1.04e-05	-3.68e-06	6.56e-06	-3.51e-06	-2.06e-06
MetOp-A	3B	286.33	-4.80e-04	1.80e-04	-3.03e-04	1.81e-04	-1.39e-03
	4	285.01	-4.74e-06	2.13e-06	-3.09e-06	2.13e-06	1.43e-06
	5	284.98	9.45e-06	-3.41e-06	5.98e-06	-3.63e-06	-2.34e-06

Table 3.1: Effective temperature residuals for a blackbody temperature of 285K between the reference AVHRR SRFs (derived from the NESDIS/STAR AVHRR SRFs [Wu, X.] via spline interpolation with tension 5.0), different interpolation methods (including none at all), and the current SRF used in CRTM processing.

[4] See appendix B for a definition of effective temperature.

4 Impact of wide SRF wings

To minimise the amount of monochromatic transmittances calculations that are required, the wings of instrument SRFs are truncated. The frequency at which this truncation occurs is somewhat subjective and requires visual inspection of the SRF wings to determine if the data is real, noise, or an artifact of the measurement system. This section is a short description of how this truncation can affect the results when an SRF has wide wings.

Generally, the truncation frequency is selected when the response values decreases below a value of 10^{-4}. In processing the NOAA-16 AVHRR/3 channel 3B data from the NESDIS/STAR website, it was noticed that the shortwave wing of the SRF extended almost two full widths at half-maximum (FWHM) (see the top panel of figure 4.1). Close inspection of this shortwave wing revealed that the data was quantised at the 10^{-3} level, and that the wing had a constant value of 0.002 from approximately 2900-3300cm^{-1} (see the bottom panel of figure 4.1). Because this value is larger than the nominal cutoff magnitude, the entire wing was included in the initial processing.

As shown in figure 4.1, frequencies were selected at which to truncate the SRF. The selected $f1$ and $f2$ cutoff frequencies for this channel were 2290cm^{-1} and 2920cm^{-1}. The impact of this truncation is shown in table 4.1 where the effective temperatures for a blackbody temperature of 285K differ by 0.13K.

SRF Type	T_{eff} (K)	ν_o (cm^{-1})	a_0 (K)	a_1 (K/K)
Original (no cutoff)	286.25	2697.5630	2.268358	0.996416
Original (with cutoff)	286.12	2696.4477	2.017304	0.996841

Table 4.1: Differences in effective temperatures, central frequencies and band correction coefficients for NOAA-16 AVHRR channel 3B due to the reported extended SRF wings. See figure 4.1.

Given the quantisation of the SRF data for NOAA-16 channel 3B, it is assumed that the wide shortwave wing is a measurement artifact and not a true representation of the SRF response.

While other AVHRR channels (on other platforms) also had wide SRF wings, their wing values were either much closer to zero (e.g., see figures 4.2 and 4.3), or clearly recognisable as measurement noise (e.g. see figure 4.4). However, there are still some SRFs that may require further analysis due the behaviour of their wings (e.g. see figure 4.5.)

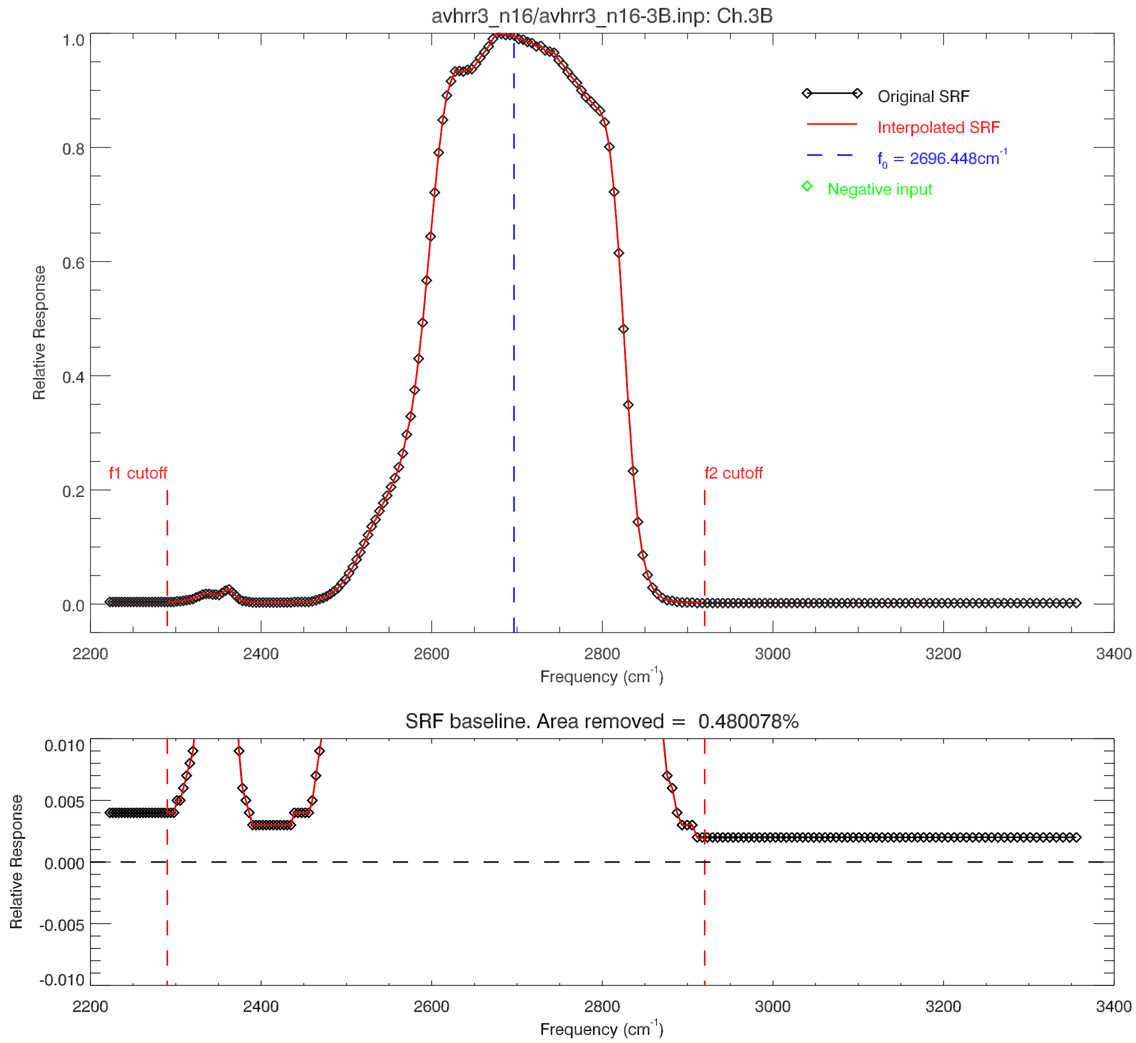

Figure 4.1: NOAA-16 AVHRR/3 channel 3B SRF indicating the frequencies at which the original SRF data was truncated prior to interpolation. **(Top panel)** The entire SRF. **(Bottom panel)** A magnification showing the elevated wings of the SRF.

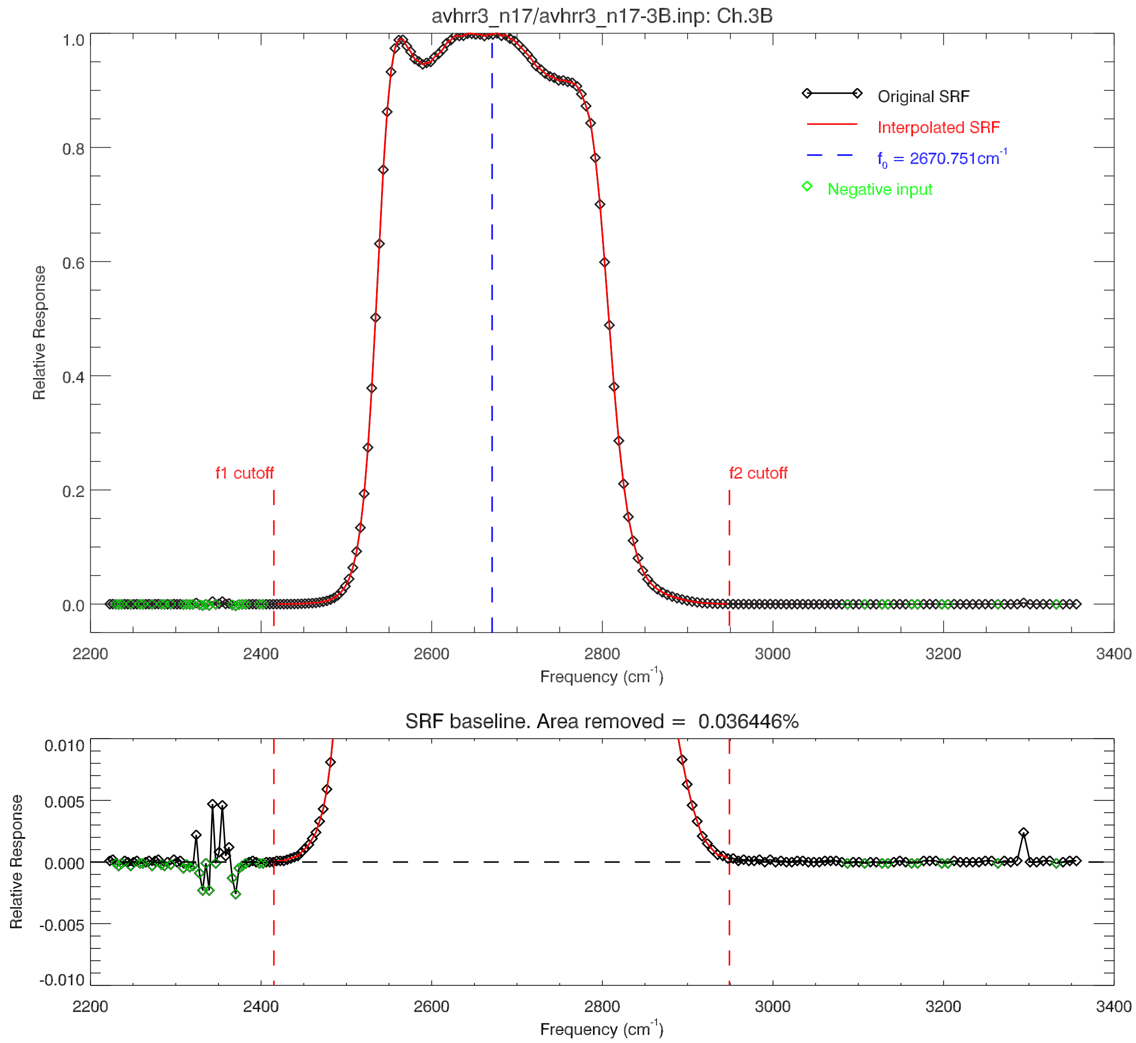

Figure 4.2: NOAA-17 AVHRR/3 channel 3B SRF indicating the frequencies at which the original SRF data was truncated prior to interpolation. **(Top panel)** The entire SRF. **(Bottom panel)** A magnification showing the wings of the SRF.

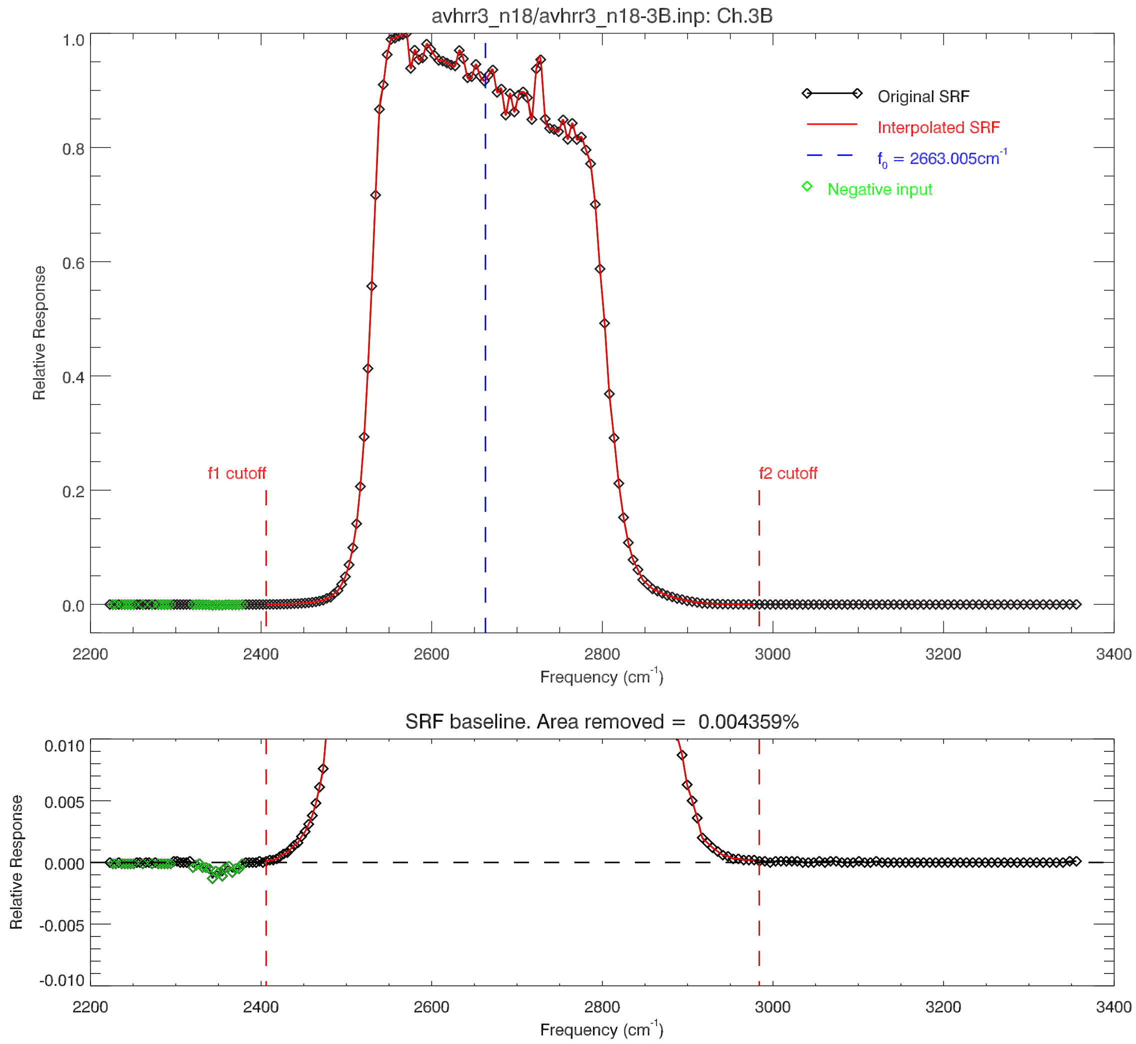

Figure 4.3: NOAA-18 AVHRR/3 channel 3B SRF indicating the frequencies at which the original SRF data was truncated prior to interpolation. **(Top panel)** The entire SRF. **(Bottom panel)** A magnification showing the wings of the SRF.

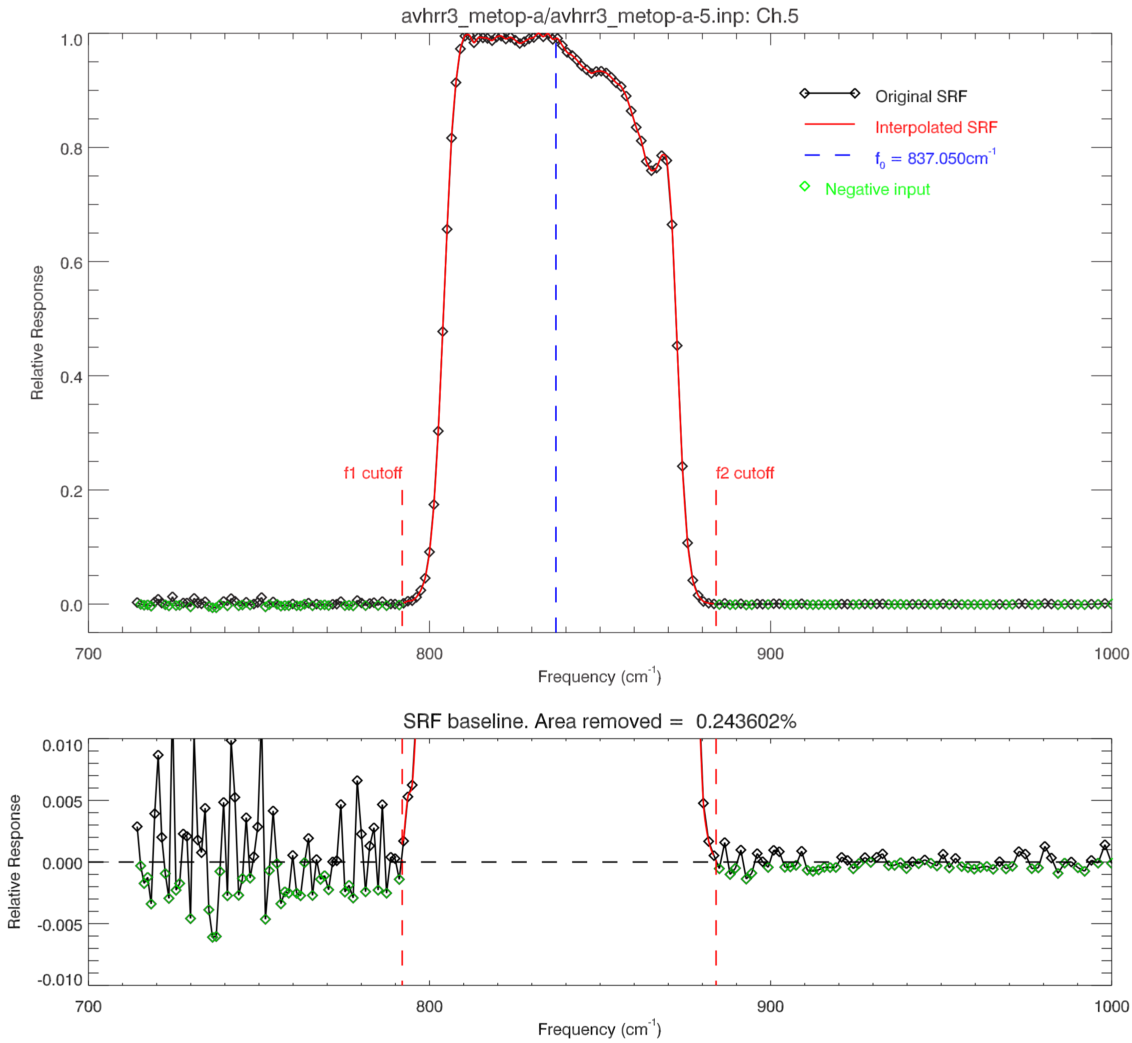

Figure 4.4: MetOp-A AVHRR/3 channel 5 SRF indicating the frequencies at which the original SRF data was truncated prior to interpolation. **(Top panel)** The entire SRF. **(Bottom panel)** A magnification showing the wings of the SRF.

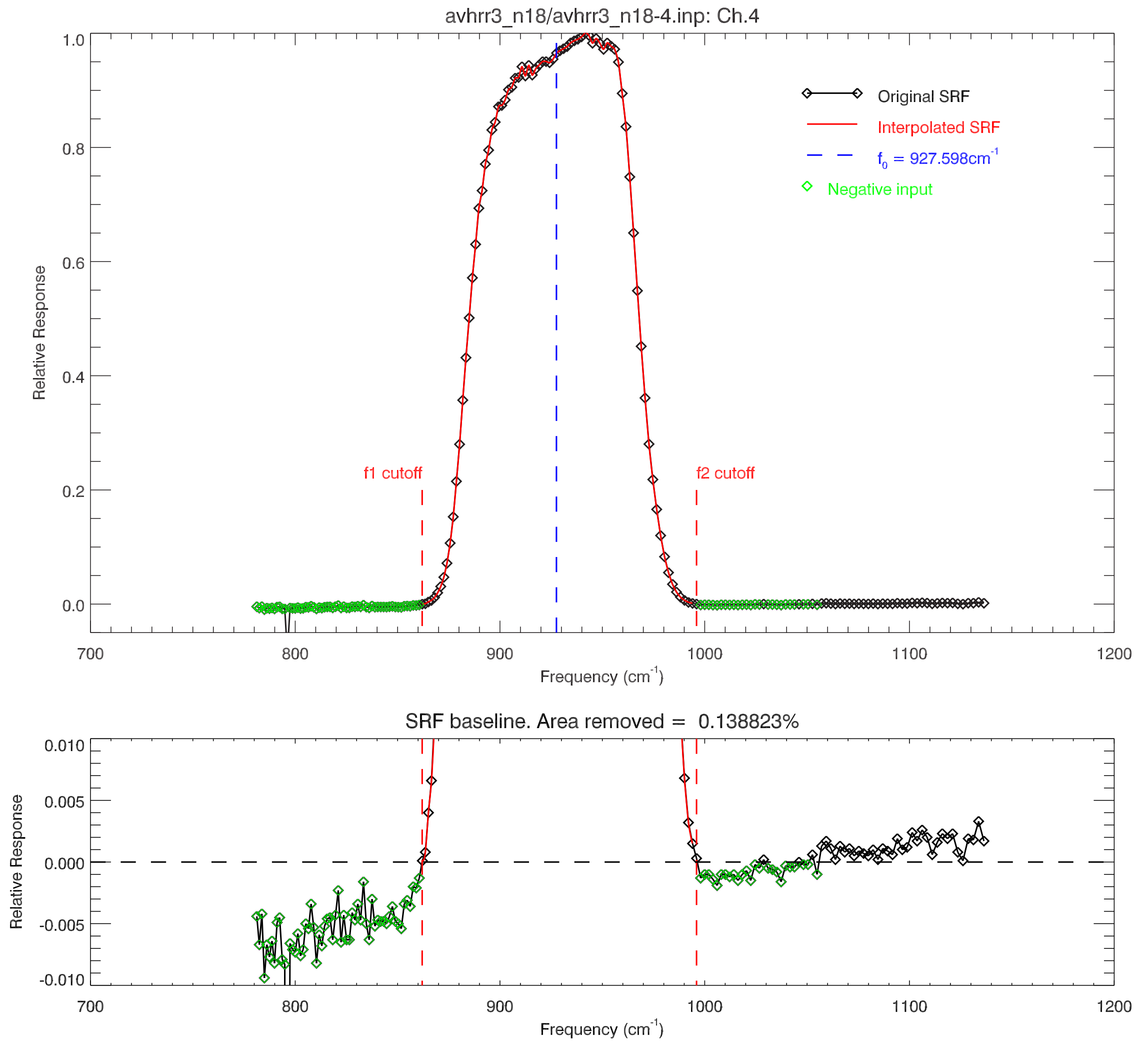

Figure 4.5: NOAA-18 AVHRR/3 channel 4 SRF indicating the frequencies at which the original SRF data was truncated prior to interpolation. **(Top panel)** The entire SRF. **(Bottom panel)** A magnification showing the wings of the SRF.

References

Sullivan, J.T. Private communication, June 2003.

Sullivan, J.T. Private communication, January 2006.

Woolf, H.M. CIMSS Spectral Response Functions. URL ftp://monkey.ssec.wisc.edu/pub/srf. Last accessed 2008-10-29.

Wu, X. NOAA AVHRR Spectral Response Functions. URL http://www.star.nesdis.noaa.gov/smcd/spb/fwu/solar_cal/spec_resp_func. Last accessed 2008-11-04.

A AVHRR infrared channel SRF comparison

The following are plots of the AVHRR/3 infrared SRF data from the NESDIS/STAR website (labeled as "Official") and those from the CIMSS/SSEC ftp site (labeled as "Current") for the four AVHRR/3 instruments onboard NOAA-16, -17, -18, and MetOp-A. The interpolated SRFs are also shown as overplots. At the scale that encompasses the entire SRF one cannot easily distinguish between the various SRFs.

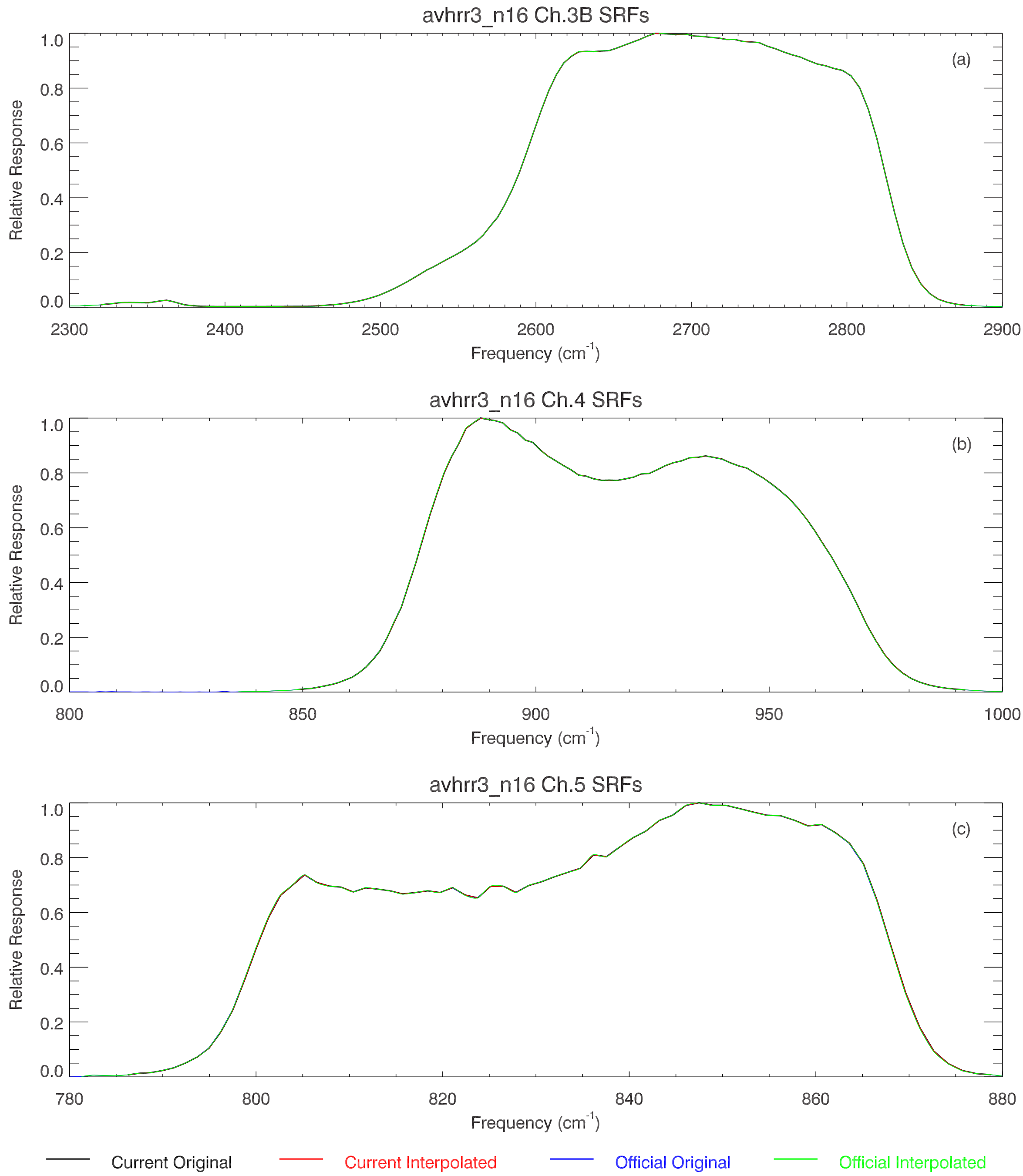

Figure A.1: Comparison of NOAA-16 AVHRR/3 Infrared channel SRFs.

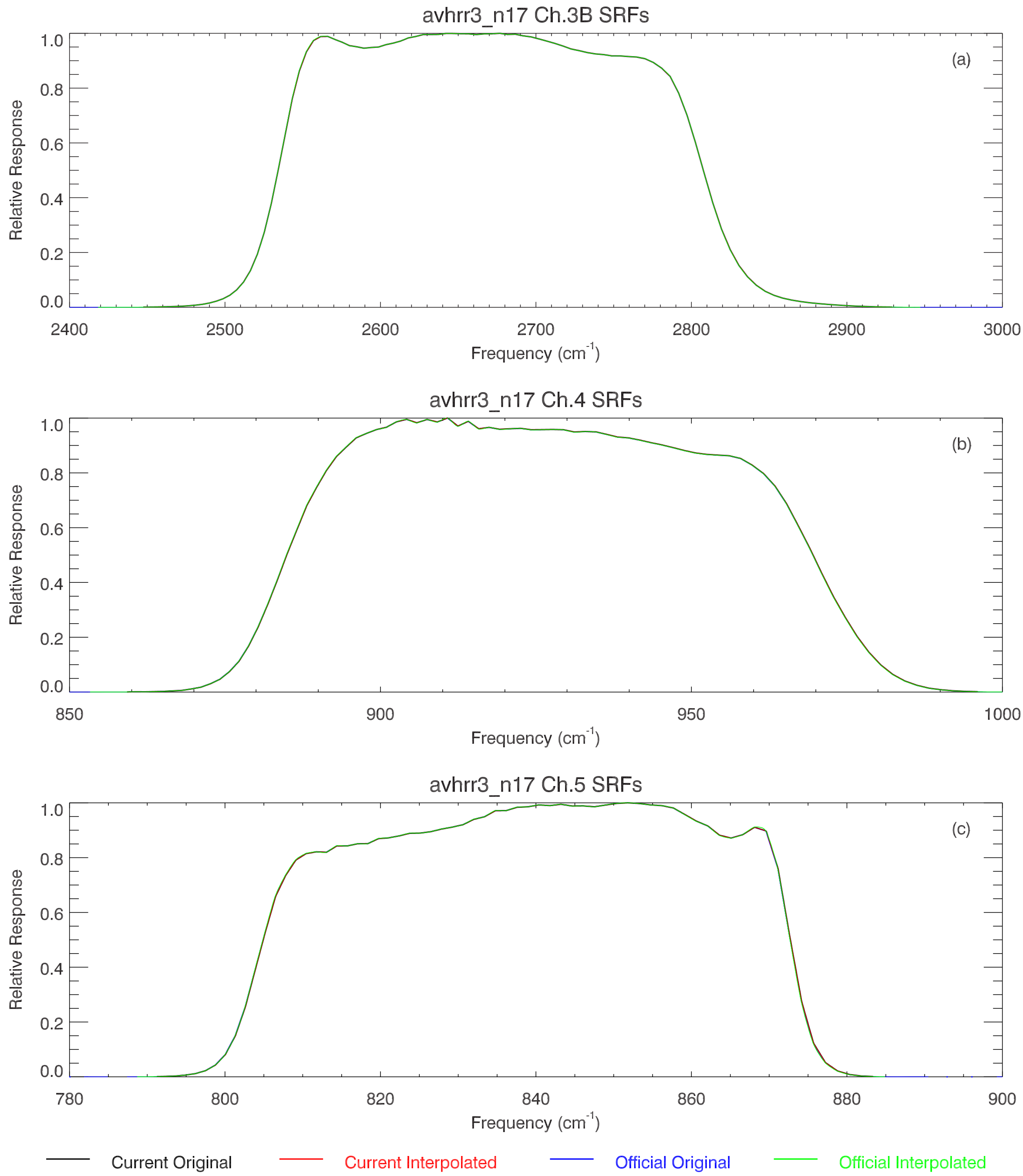

Figure A.2: Comparison of NOAA-17 AVHRR/3 Infrared channel SRFs.

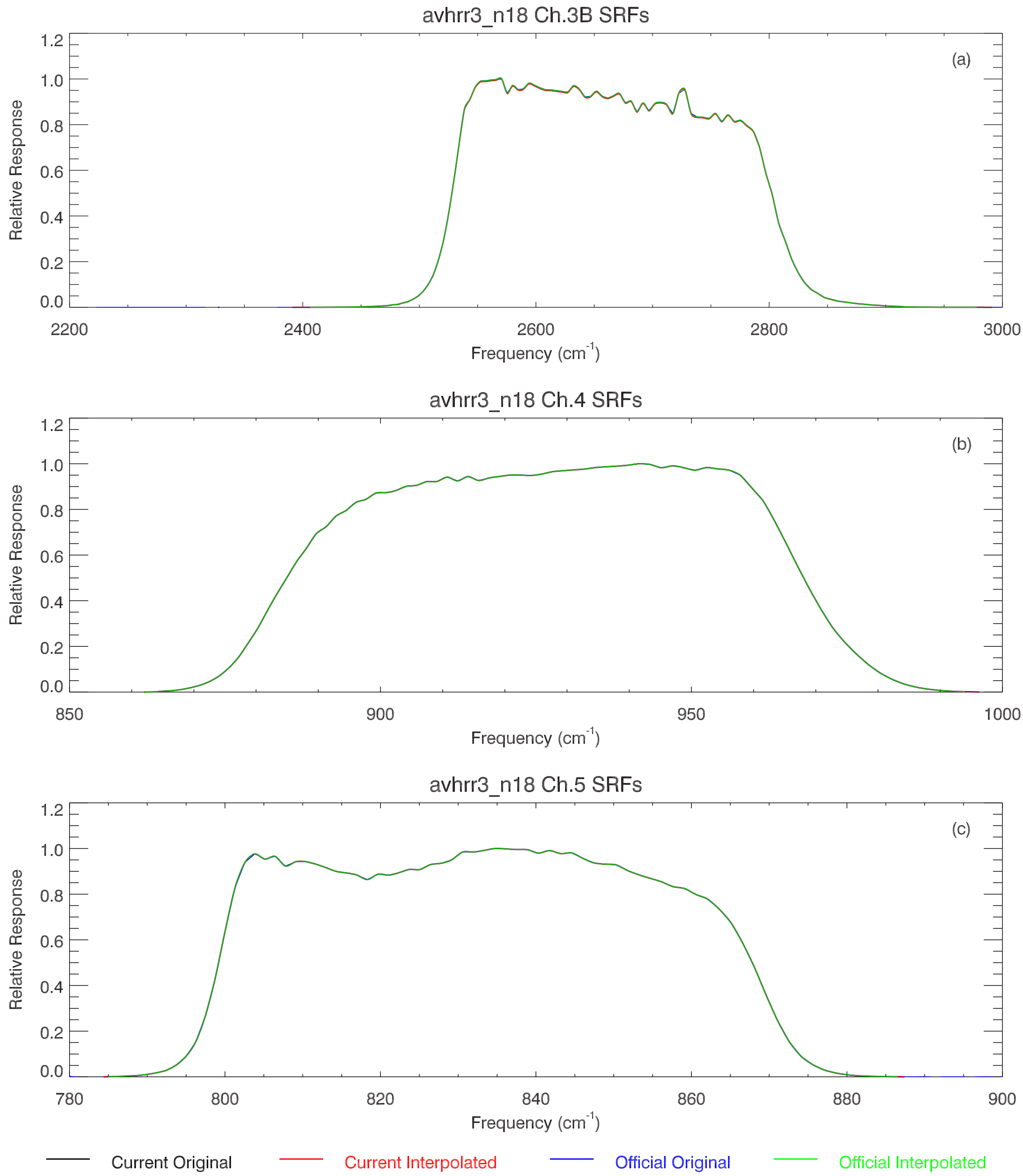

Figure A.3: Comparison of NOAA-18 AVHRR/3 Infrared channel SRFs.

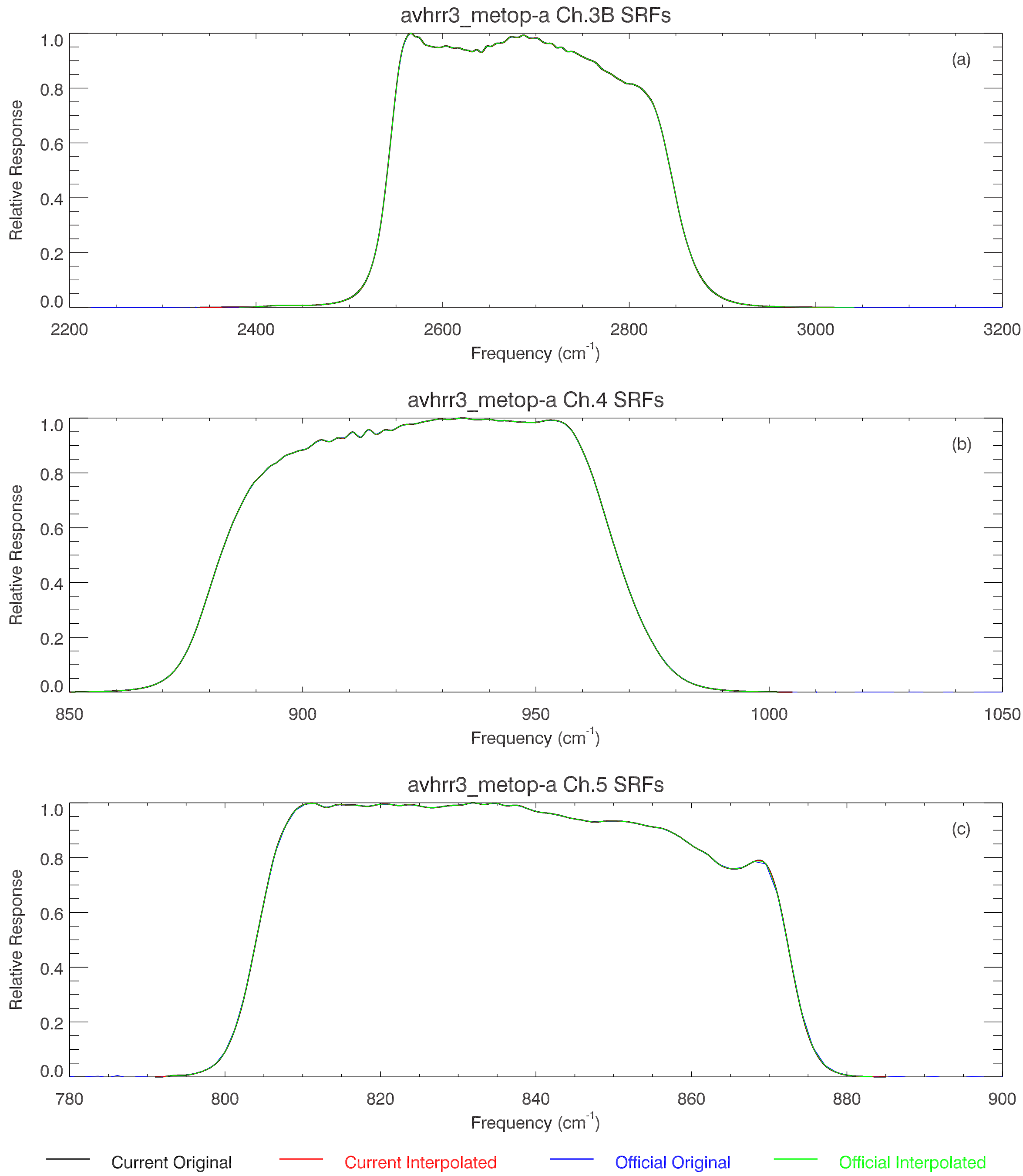

Figure A.4: Comparison of MetOp-A AVHRR/3 Infrared channel SRFs.

B AVHRR infrared channel band correction coefficients

To account for broadband channel polychromaticity in Planck calculations in the CRTM, we assume the true temperature, T, is related to a channel (or effective) temperature, T_{eff}, via a simple polynomial relationship,

$$\sum_{i=0}^{N} a_i \cdot T^i = \frac{c_1 \nu_o^3}{\ln\left[\dfrac{c_2 \nu_o}{R(T)} + 1\right]} = T_{eff} \tag{B.1}$$

Here the a values are the "band correction" coefficients, ν_o is the channel central frequency determined from the first moment of the defined spectral response, $\Phi(\nu)$,

$$\nu_o = \frac{\int_{\nu_1}^{\nu_2} \nu \Phi(\nu) d\nu}{\int_{\nu_1}^{\nu_2} \Phi(\nu) d\nu} \tag{B.2}$$

and $R(T)$ is the channel blackbody radiance determined by convolving the monochromatic Planck radiance with the spectral response,

$$R(T) = \frac{\int_{\nu_1}^{\nu_2} B(T, \nu) \Phi(\nu) d\nu}{\int_{\nu_1}^{\nu_2} \Phi(\nu) d\nu} \tag{B.3}$$

Solving equation B.1 then yields the a coefficients. For the CRTM, we use a simple linear fit ($N = 1$) for a temperature range of 180-340K to yield two band correction coefficients for each channel.

The central frequencies and band correction coefficients presented in this appendix were derived using the official AVHRR SRFs from the NESDIS/STAR website [Wu, X.] and their various derived interpolates, and the current SRF used in the CRTM processing.

SRF Type	Channel	ν_o (cm^{-1})	a_0 (K)	a_1 (K/K)
	3B	2696.4477	2.017304	0.996841
Spline5	4	918.1333	0.467188	0.998382
	5	835.8874	0.246714	0.999068
	3B	2696.4512	2.018046	0.996840
Linear	4	918.1346	0.467384	0.998382
	5	835.8893	0.246845	0.999067
	3B	2696.4445	2.016995	0.996841
Spline0.1	4	918.1323	0.467111	0.998383
	5	835.8863	0.246661	0.999068
	3B	2696.4503	2.017781	0.996840
Spline20	4	918.1342	0.467313	0.998382
	5	835.8887	0.246798	0.999067
	3B	2696.4440	2.017148	0.996841
Original	4	918.1322	0.467111	0.998383
	5	835.8863	0.246651	0.999068
	3B	2696.6687	1.937532	0.997018
Current	4	918.1837	0.463810	0.998394
	5	835.9503	0.246092	0.999070

Table B.1: Central frequencies and band correction coefficients for the NOAA-16 AVHRR.

SRF Type	Channel	ν_o (cm^{-1})	a_0 (K)	a_1 (K/K)
	3B	2670.7506	1.725340	0.997705
Spline5	4	926.9926	0.380521	0.998693
	5	839.3402	0.227473	0.999145
	3B	2670.7541	1.726104	0.997704
Linear	4	926.9938	0.380728	0.998693
	5	839.3410	0.227614	0.999144
	3B	2670.7480	1.725069	0.997705
Spline0.1	4	926.9916	0.380443	0.998694
	5	839.3395	0.227420	0.999145
	3B	2670.7532	1.725820	0.997704
Spline20	4	926.9935	0.380653	0.998693
	5	839.3408	0.227563	0.999144
	3B	2670.7480	1.725070	0.997705
Original	4	926.9916	0.380444	0.998694
	5	839.3394	0.227421	0.999145
	3B	2670.8000	1.725090	0.997705
Current	4	927.0426	0.380562	0.998693
	5	839.3913	0.227577	0.999144

Table B.2: Central frequencies and band correction coefficients for the NOAA-17 AVHRR.

SRF Type	Channel	ν_o (cm^{-1})	a_0 (K)	a_1 (K/K)
	3B	2663.0046	1.762539	0.997675
Spline5	4	927.5976	0.374180	0.998715
	5	833.2219	0.240701	0.999089
	3B	2663.0082	1.763299	0.997674
Linear	4	927.5987	0.374387	0.998714
	5	833.2228	0.240837	0.999089
	3B	2663.0019	1.762274	0.997675
Spline0.1	4	927.5967	0.374101	0.998715
	5	833.2213	0.240650	0.999089
	3B	2663.0072	1.763015	0.997674
Spline20	4	927.5984	0.374312	0.998714
	5	833.2226	0.240787	0.999089
	3B	2663.0020	1.762273	0.997675
Original	4	927.5965	0.374105	0.998715
	5	833.2212	0.240652	0.999089
	3B	2663.0040	1.762689	0.997675
Current	4	927.5991	0.374231	0.998715
	5	833.2215	0.240707	0.999089

Table B.3: Central frequencies and band correction coefficients for the NOAA-18 AVHRR.

SRF Type	Channel	ν_o (cm^{-1})	a_0 (K)	a_1 (K/K)
	3B	2689.9372	2.128139	0.997208
Spline5	4	926.1051	0.386193	0.998672
	5	837.0500	0.228639	0.999139
	3B	2689.9409	2.128900	0.997207
Linear	4	926.1064	0.386395	0.998671
	5	837.0512	0.228773	0.999138
	3B	2689.9344	2.127868	0.997208
Spline0.1	4	926.1041	0.386115	0.998672
	5	837.0492	0.228588	0.999139
	3B	2689.9399	2.128616	0.997207
Spline20	4	926.1060	0.386321	0.998671
	5	837.0508	0.228724	0.999138
	3B	2689.9344	2.127864	0.997208
Original	4	926.1042	0.386114	0.998672
	5	837.0493	0.228586	0.999139
	3B	2689.8937	2.132029	0.997199
Current	4	926.1043	0.386139	0.998672
	5	837.0496	0.228604	0.999139

Table B.4: Central frequencies and band correction coefficients for the MetOp-A AVHRR.